

**Title: Laser induced ultrafast 3d and 4f spin dynamics in CoDy ferrimagnetic alloys as a function of temperature.**

T. Ferté<sup>1</sup>, N. Bergeard<sup>1\*</sup>, G. Malinowski<sup>2</sup>, E. Terrier<sup>1</sup>, V. Halté<sup>1</sup>, L. Le Guyader<sup>3</sup>, K. Holldack<sup>3</sup>, M. Hehn<sup>2</sup> and C. Boeglin<sup>1</sup>

<sup>1</sup> *Université de Strasbourg, CNRS, Institut de Physique et Chimie des Matériaux de Strasbourg, UMR 7504, F-67000 Strasbourg, France.*

<sup>2</sup> *Institut Jean Lamour, Université de Lorraine, BP 50840, 54011 Nancy, France*

<sup>3</sup> *Institut für Methoden und Instrumentierung der Forschung mit Synchrotronstrahlung Helmholtz-Zentrum Berlin für Materialien und Energie GmbH, Albert-Einstein-Str. 15, 12489 Berlin, Germany*

\* *Corresponding author:*

*Mel: [nicolas.bergeard@ipcms.unistra.fr](mailto:nicolas.bergeard@ipcms.unistra.fr)*

*Address: Institut de Physique et de Chimie des Matériaux de Strasbourg (IPCMS)  
Campus Cronenbourg 23 rue du Loess BP43 67034 Strasbourg*

## **0. Abstract**

We report on an element- and time-resolved investigation of femtosecond laser induced ultrafast dynamics of 3d and 4f spins in a ferrimagnetic Co<sub>80</sub>Dy<sub>20</sub> alloy as a function of temperature. We observe an increase of the Co3d characteristic demagnetization time and a decrease of the Dy4f demagnetization time when the temperature is approaching the Curie temperature. It suggests that the “critical slowing down” regime, which affects the laser induced ultrafast dynamics in pure 3d transition metals and 4f rare-earth ferromagnetic layers, vanishes for the Dy sublattice in the CoDy alloy, in line with the theoretical predictions of the Landau-Lifshitz-Bloch (LLB) model.

*Key words:*

**Ferrimagnetic alloys, ultrafast laser induced demagnetization, femtosecond laser, time-resolved X-ray Magnetic Circular Dichroism.**

## 1. Introduction

Excitation of ferromagnetic layers with infra-red (IR) femtosecond (fs) laser pulses leads to a quenching of the magnetic order on a sub-picosecond time scale [BEA96]. The microscopic mechanisms that govern this ultrafast demagnetization are still subject to controversy in spite of intensive experimental and theoretical studies [KOO10, BAT10, CAR11, ESS12, CAR13, SCH13, SHO17]. Although these investigations have revealed fundamental dissimilarities in the laser induced ultrafast magnetization dynamics in transition metals (TM) [BEA96, STA07, KUI11, ROT12] and in rare-earth (RE) layers [WIE11, SUL12, ESC14, FRI15, RET16], some general features were established. For instance, the Curie temperature ( $T_{\text{Curie}}$ ) is known to play an important role. Indeed, the characteristic quenching times ( $\tau$ ) of the 3d magnetic order in transition metals (TM) and 5d magnetic order in pure rare-earth (RE) layers are known to increase when the temperature is approaching  $T_{\text{Curie}}$  due to the so-called “critical slowing down” (CSD) [CHU06, SUL12, MEN14]. This “slowing down” of dynamics is expected in second order phase transitions [KIS00] and may originate from the magnon softening [MAN12] or the divergence of the magnetic heat capacity [KIM14] in the vicinity of  $T_{\text{Curie}}$ . Among the various theoretical models proposed so far to explain the origin of laser induced ultrafast demagnetization [KOO10, BAT10], the Landau-Lifshitz-Bloch (LLB) models allows to reproduce the divergence of  $\tau$  in the vicinity of  $T_{\text{Curie}}$  for both pure TM [CHU06] and pure RE [SUL12] layers. In the specific case of pure RE layers, the CSD has been experimentally observed for the itinerant 5d magnetic moments by means of tr-MOKE [SUL12]. The LLB model predicts that the CSD affects also the laser induced dynamics of localized 4f spins [SUL12]. Such prediction is sustained by experiments that have evidenced concomitant laser induced dynamics of the 5d and 4f spins [WIE11, SUL12, SUL12a, ESC14, RET16, BOB17].

To go beyond the description of spin dynamics in ferromagnetic layers, the LLB model was extended to treat the laser induced ultrafast dynamics in multi-sublattices ferrimagnetic alloys [ATX12] such as FeCoGd [ATX14], CoTb [MOR17] and FeTb [MOR19] alloys. This extension have allowed to address specifically the 3d and 4f spin dynamics in FeCoGd alloys and in the vicinity of  $T_{\text{Curie}}$  [ATX14]. In this theoretical study, the authors predicted that the CSD does not occur for Gd4f spins in the vicinity of  $T_{\text{Curie}}$  while it still affects the dynamics of the FeCo3d spins. The authors stated that the Gd4f spin dynamics is dominated by antiferromagnetic spin fluctuations that are temperature independent while the FeCo3d spin dynamics is dominated by

ferromagnetic spin fluctuations that are sensitive to the CSD regime. In this framework, the characteristic demagnetization time of the FeCo sublattice ( $\tau_{\text{FeCo}}$ ) diverges at  $T_{\text{Curie}}$ , while the characteristic demagnetization time of the Gd sublattice ( $\tau_{\text{Gd}}$ ) remains finite. However, there are no conclusive experimental evidences to corroborate these predictions [RAD11, LOP13, GRA13, BER14, RAD15, HIG16, FER17]. Radu et al. have empirically established a linear relation between  $\tau$  and  $m$ , the magnetic moment, in different RE-TM alloys [RAD15] which would be consistent with a reduction of  $\tau_{\text{Gd}}$  when the temperature is approaching  $T_{\text{Curie}}$ . However, the LLB model states that such proportionality between  $\tau$  and  $m$  fails at high temperature [ATX14]. Ferté et al. have investigated laser induced demagnetization in  $\text{Co}_{80}\text{Dy}_{20}$  and  $\text{Co}_{78}\text{Dy}_{22}$  alloys at two different temperatures but for a constant  $|T - T_{\text{Curie}}|$  [FER17]. They showed similar characteristic demagnetization times for both the Co and Dy sublattices. Although this first set of data is in agreement with the LLB model, experiments at various  $|T - T_{\text{Curie}}|$  values are required to challenge the LLB model predictions.

In this work, we have studied the laser induced ultrafast dynamics of Co3d and Dy4f spins in a  $\text{Co}_{80}\text{Dy}_{20}$  ferrimagnetic alloy for three different temperatures by mean of time-resolved X-Ray Magnetic Circular Dichroism (tr-XMCD) [HOL14]. Interestingly, we show that  $\tau_{\text{Co}}$  increases while  $\tau_{\text{Dy}}$  decreases when the temperature rises towards  $T_{\text{Curie}}$  confirming the predictions of the LLB model. Thus, we conclude that the characteristic demagnetization times of both the Co3d and Dy4f sublattices depend on  $|T - T_{\text{Curie}}|$ .

## 2. *Material and methods*

The 18 nm thick  $\text{Co}_{80}\text{Dy}_{20}$  alloy layer was deposited by DC magnetron sputtering on a “heat sink” Ta(3)/Cu(20)/Ta(3) multilayer sustained by a  $\text{Si}_3\text{N}_4$  membrane. The alloy was capped with a Al(3)/Ta(3) bi-layer to prevent oxidization. We measured hysteresis loops at various temperatures using SQUID magnetometry to extract the dependence of the saturation field ( $H_{\text{sat}}$ ) on temperature (figure 1). As expected, the  $\text{Co}_{80}\text{Dy}_{20}$  alloy displays out-of-plane magnetic anisotropy and  $H_{\text{sat}}$  diverges at  $T \sim 250\text{K}$  which is the temperature of magnetic compensation ( $T_{\text{comp}}$ ) [BIN06, STA06]. These measurements show that the alloy can be saturated under a magnetic field of 0.55 T (horizontal dotted line on figure 1) for  $T < 160\text{ K}$  and  $T > 300\text{ K}$ .

The tr-XMCD experiments were carried out at the femtoslicing beam line of the BESSY II synchrotron radiation source at the Helmholtz-Zentrum Berlin [HOL14]. The configuration of the pump-probe experiments was the same as in our previous work [FER17]. The magnetization dynamics have been measured by monitoring the transmission of circularly polarized X-ray pulses tuned to specific core level absorption edges as a function of a pump-probe delay for two opposite directions of the magnetic field. The photon energy was set to the CoL<sub>3</sub> and the DyM<sub>5</sub> edges using a reflection zone plate monochromator on UE56/1-ZPM. The 800nm pump laser diameter was set to 500 μm to ensure homogeneous pumping over the probed area of the sample (~200 μm). A magnetic field of ±0.55 T was applied along the propagation axis of both the IR laser and the X-ray beam during the experiment. The measurements were carried out at  $T^* = 350$  K (configuration 1), 400 K (configuration 2) and 540 K (configuration 3) with  $T^* = T_C - (T_{\text{cryo}} + \Delta T)$  as illustrated in figure 2.  $T_{\text{cryo}}$  is the temperature of the cryostat and  $\Delta T$  is the temperature elevation due to the laser continuous heating (table 1). The Curie temperature of the Co<sub>80</sub>Dy<sub>20</sub> alloy ( $T_{\text{Curie}} = 700$  K) is extrapolated from literature [HAN91] and from mean field calculations [MAN86, BER17]. As only one single sample was used in this experiment, any small error on the estimated value of  $T_{\text{Curie}}$  would shift  $T^*$  without affecting our conclusions. The experimental parameters, such as the pump laser powers ( $P$ ) and  $T_{\text{cryo}}$ , have been chosen so that  $T_{\text{cryo}} + \Delta T$  was either below 160 K or above 300 K (figure 1) [BIN06, STA06] to allow for magnetic saturation of our alloy under the magnetic field of 0.55T. We relied on the thermal variation of the saturation field (figure 1) to determine  $\Delta T$  for the two different pump laser powers ( $P = 17$  and 50 mW) we have used during the experiment. To do so, we initially set  $T_{\text{cryo}} = 80$  K and turned on the laser.  $P = 17$  mW was the largest laser power for which  $T_{\text{cryo}} + \Delta T$  stays below  $T = 160$ K. Above this temperature, the CoDy alloy could not be saturate (figure 1). As a consequence, we have estimated that  $\Delta T \sim 80$  K for  $P = 17$ mW. In order to estimate  $\Delta T$  with  $P = 50$  mW, we have compared the hysteresis loops at  $T_{\text{cryo}} = 300$  and 320 K with  $P = 0$  mW to the hysteresis loops recorded at negative delay for  $T_{\text{cryo}} = 80$ K with  $P = 50$  mW (figure 3). The same signs of the hysteresis loops indicate that the measurements were performed above  $T_{\text{comp}}$  for the 3 cases. Moreover, we notice that the saturation field is smaller for  $P = 50$ mW and  $T_{\text{cryo}} = 80$ K compared to  $P = 0$  mW and  $T_{\text{cryo}} = 300$  and 320 K. According to the thermal variation of the saturation field above  $T_{\text{comp}}$  (figure 1), we estimated that  $T_{\text{cryo}} + \Delta T$  is above 320K for  $P = 50$ mW and  $T_{\text{cryo}} = 80$ K. The shape of the hysteresis loop at  $P = 50$ mW and  $T_{\text{cryo}} = 80$ K also indicates that we are approaching the temperature of spin reorientation transition [DON17]. As a consequence, we have estimated  $\Delta T > 250$  K for  $P = 50$  mW. Obviously, our procedure to estimate  $\Delta T$  results in significant error bars on  $T^*$  (figure 5). Nevertheless, we

estimated that we performed the time-resolved experiments at  $T^* = 350$  K, 400 K and 540 K (figure 2, table 1). The measurements were carried out above  $T_{\text{comp}}$  for the configurations 1 and 2 (figure 2a and b) and below  $T_{\text{comp}}$  for the configurations 3 (figure 2c) [FER17].

### 3. *Experimental results and discussion*

The normalized transient XMCD signals recorded at the Co  $L_3$  and Dy  $M_5$  edges for  $T^* = 350$ , 400 and 540 K are displayed in figure 4a, b and c respectively. At  $T^*=540$ K (figure 4c), the maximum demagnetization of the Co sublattice is reached while the demagnetization of the Dy sublattice has barely started as reported in a large number of element- and time-resolved experiments for different RE-TM alloys [RAD11, LOP13, GRA13, RAD15, HIG16, FER17]. Oppositely, at  $T^* = 350$ K (figure 4a), the magnetization of the Dy sublattice is close to its minimum value when the minimum magnetization of the Co sublattice is reached. The tr-XMCD curves at the Co  $L_3$  edges were adjusted with two exponential functions (respectively the demagnetization and the magnetization recovery) convoluted by a Gaussian function to account for the experimental time resolution (130 fs) [BOE10, LOP12, BER14]. It is worth noticing that we have imposed a lower limit at 130 fs for the characteristic demagnetization times during the fitting procedure. It means that the actual  $\tau_{\text{Co}}$  is possibly below the experimental time resolution for  $T^* = 400$  K and 540K. The tr-XMCD curves at the Dy  $M_5$  edge were adjusted by a single exponential decay convoluted by a Gaussian function since we did not observe any recovery on the recorded time range. We have extracted the characteristic demagnetization times ( $\tau$ ) from these adjustments as well as their error bars, which correspond to the standard deviation (table 1). The dependence of the characteristic demagnetization times on temperature for both sublattices are displayed in figure 5. We also report the characteristic demagnetization times for the Co and Dy sublattices in various CoDy alloys measured by Ferté et al (in  $\text{Co}_{80}\text{Dy}_{20}$  and  $\text{Co}_{78}\text{Dy}_{22}$ ) [FER17] and Radu et al (in  $\text{Co}_{83}\text{Dy}_{17}$ ) [RAD15] in figure 6. Ferté et al have explicitly given the numerical values for  $T_{\text{cryo}}$ ,  $T_{\text{Curie}}$  and  $\Delta T$  [FER17] and therefore we have derived  $T^* = 430$  and 450K for the  $\text{Co}_{80}\text{Dy}_{20}$  and  $\text{Co}_{78}\text{Dy}_{22}$  alloys respectively. Radu et al have performed their measurements at  $T = 100$ K but they haven't explicit any temperature elevation due to the laser DC heating. Therefore, we assumed that  $\Delta T = 0$ K in their case and we derived  $T^*=930$ K since  $T_{\text{Curie}} = 1030$ K for their  $\text{Co}_{83}\text{Dy}_{17}$  alloys [DON17].

*Table 1: Parameters extracted from the fit functions.*

$T^*$ (K)	$T_{\text{Cryo}}$ (K)	$\Delta T$ (K)	Laser power (mW)	Edge	Demagnetization time $\tau$ (fs)
540	80	80	17	Co $L_3$	$130 \pm 100$
540	80	80	17	Dy $M_5$	$980 \pm 200$
400	220	80	17	Co $L_3$	$130 \pm 60$
400	220	80	17	Dy $M_5$	$570 \pm 90$
350	80	> 250	50	Co $L_3$	$212 \pm 25$
350	80	> 250	50	Dy $M_5$	$400 \pm 100$

In figure 5, we observe an increase of  $\tau_{\text{Co}}$  as we approach  $T_{\text{Curie}}$  ( $T^* = 350\text{K}$ ). This increase at  $T^* = 350\text{K}$  could be even more pronounced considering that  $\tau_{\text{Co}}$  is probably overestimated at  $T^* = 400$  and  $540\text{K}$  due to the limited experimental time-resolution of 130 fs. This increase of  $\tau_{\text{Co}}$  in the vicinity of  $T_{\text{Curie}}$  could be related to the larger demagnetization amplitude induced by the larger laser power used ( $P = 50\text{mW}$  instead of  $P = 17\text{mW}$ ) [KUI11, ROT12]. However, we ruled out such explanation since Jal et al have shown that  $\tau_{\text{Co}}$  does not depend on the laser power in CoDy alloys [JAL19]. Thus, we suggest that the larger value of  $\tau_{\text{Co}}$  at  $T^* = 350\text{K}$  could be the signature of the CSD regime as predicted by the LLB model [ATX14]. However, our experimental data do not allow definitive conclusions especially if we consider the numerical values of  $\tau_{\text{Co}}$  extracted from figure 6.

Considering the ultrafast dynamics of the Dy sublattice, we observe a clear decrease of  $\tau_{\text{Dy}}$  in our alloy when the temperature is approaching  $T_{\text{Curie}}$  (figure 5). This behavior is corroborated by literature (figure 6). In pure Gd layer, the characteristic demagnetization time  $\tau_{\text{Gd}}$  related to the (5d, 6s) magnetic order increases when the fluence of the laser is increased [SUL12, FRI16]. The concomitant quenching of itinerant (5d, 6s) and localized 4f magnetic order in pure RE layers [WIE11, SUL12, ESC14, RET16, BOB17] suggest that such increase is also expected for the 4f spins. Such behavior is not observed in our alloy since the shorter demagnetization time is obtained for the larger laser power and thus the larger demagnetization amplitude. Therefore, we can rule out the distinct laser power as the origin of the measured variation of  $\tau_{\text{Dy}}$  with temperature. Gang et al. have reported a decrease of the Ni 3d characteristic

demagnetization time in NiPd ferromagnetic alloys when the Curie temperature is reduced (and thus  $T^*$ ) by increasing the Pd content [GAN18]. They have attributed such feature to the increase of the spin-flip scattering probability [KOO10] with Pd content cause by its larger spin-orbit coupling compare to pure Ni. In our case, this explanation does not hold since we have used a single alloy composition. Instead, we state that the temperature dependences of  $\tau_{\text{Co}}$  and  $\tau_{\text{Dy}}$  are consistent with the predictions of the LLB models [ATX14]. Therefore, our experimental findings support the LLB predictions and call for further experiments at higher temperature to check whether  $\tau_{\text{Co}}(T)$  and  $\tau_{\text{Dy}}(T)$  can truly be defined by the rate of magnetization change with temperature [ATX14]. Following the statement of Atxitia et al, it is of the upper fundamental interests since it would give a direct connexion between the features of laser induced ultrafast dynamics and static magnetic properties of the alloys [ATX14]. However, recent experiments have evidenced a CSD regime in an antiferromagnetic CoO layer in the vicinity of the Néel temperature [ZHE18]. These results cast doubt on the temperature independent antiferromagnetic fluctuations regime invoked by Atxitia et al to explain the vanishing of the CSD regime for the Gd4f sublattice [ATX14]. Since then, Atxitia et al have predicted, in the framework of the LLB model, that high magnetic fields may lift-off the CSD at high temperature and speed up the dynamics for pure rare-earth layers [ATX18]. This mechanism is efficient for pure RE layer because high magnetic fields strongly affect the spin-wave spectrum [HAA14] and thus the dynamics of 4f spins [AND15]. Oppositely, the dynamics of 3d spins in TM is presumably caused by spin-flip scattering [GOR18] which are not affected by large magnetic fields [HAA14]. Then, we suggest that the antiferromagnetic molecular field generated by the surrounding Co 3d spins [BRO91] could hinder the CSD for the Dy 4f spins. It could also explain why only type I dynamics was reported so far for RE4f spins in RE-TM alloys [RAD11, LOP13, GRA13, BER14, RAD15, HIG16, FER17, FER17b, FER19, HEN19]. We are looking forwards the future derivation of the LLB equations at high magnetic field and at high temperature for the specific case of ferrimagnetic alloys [ATX18].

#### ***4. Conclusions***

We have investigated the laser induced ultrafast dynamics of Co 3d and Dy 4f spins in a ferrimagnetic CoDy alloy as a function of temperature by element and time-resolved XMCD. We have evidenced that the characteristic demagnetization time of the Dy4f sublattice decreases

while the characteristic demagnetization time of the Co3d sublattice increases when the temperature is approaching the Curie temperature. Our experimental findings sustain some of the predictions of the LLB model regarding the dependence of laser induced ultrafast 3d and 4f spin dynamics on the explored temperature range. It is worth noticing that the LLB model and the microscopic 3 temperatures model [KOO10] are equivalent [ATX11]. Therefore, we expect similar conclusions from the latter theoretical model [SCH13]. Our experimental findings strongly suggest that the CSD regime affects only the 3d spin dynamics in RE-TM ferrimagnetic alloys. Since the distinct dynamics of 3d and 4f spins is believed to be the key ingredient for ultrafast all optical switching [RAD11, XU17] as well as ultrafast spin-transfer torque assisted switching [IIA18] in RE-TM alloys, it is of paramount importance to determine the correlation between the characteristic demagnetization times and physical parameters as the temperature. Furthermore, this experimental verification would give a connexion between the characteristics of laser induced ultrafast dynamics and the static magnetic properties of ferrimagnetic alloys [ATX14]. The richness and diversity of laser induced ultrafast dynamics in ferrimagnetic alloys are still not fully explored. We hope this work will motivate further experimental investigation at elevated temperatures as well as development of the LLB model to ferrimagnetic alloys [ATX18].

**Figures:**

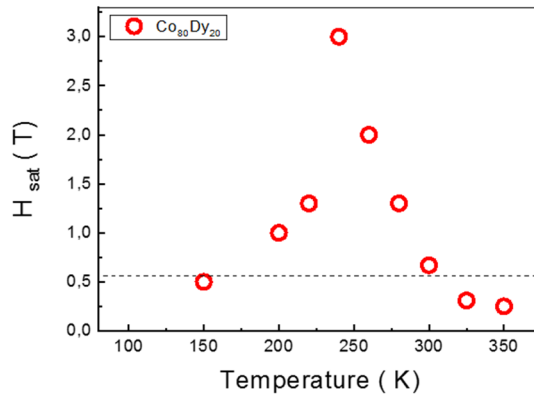


Figure 1: Saturation field as a function of temperature acquired by using a SQUID magnetometer on a Al(3)/Ta(3)/Co<sub>80</sub>Dy<sub>20</sub>(20)/Ta(3)/Ta(20)/Ta(3)/Si multilayer.

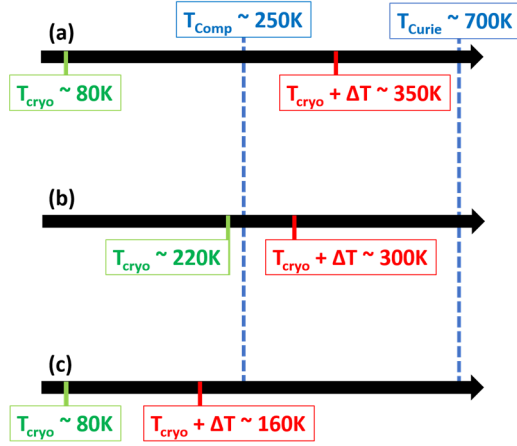


Figure 2: Sketch of the experimental conditions to reach  $T^* = 350\text{K}$  (a),  $400\text{K}$  (b) and  $540\text{K}$  (c).

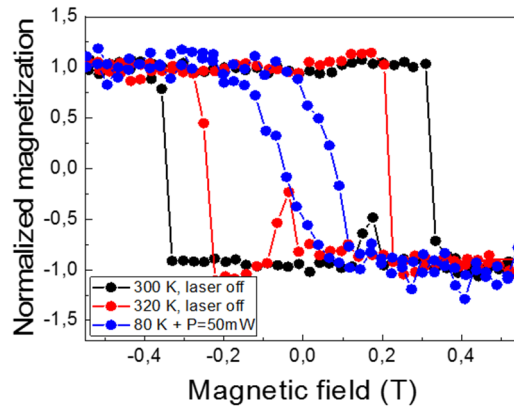


Figure 3: Hysteresis loops recorded by monitoring the X-ray transmission at the Dy  $M_5$  absorption edge as a function of the magnetic field. The experimental configurations were  $P = 0\text{mW}$  and  $T_{\text{cryo}} = 300\text{K}$  (black circles),  $P = 0\text{mW}$  and  $T_{\text{cryo}} = 320\text{K}$  (red circles) and  $P = 50\text{mW}$  and  $T_{\text{cryo}} = 80\text{K}$  (black circles).

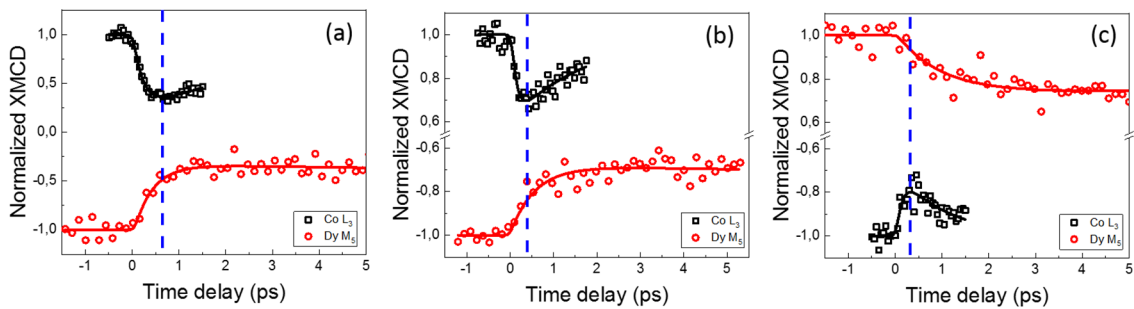


Figure 4: Transient XMCD at the Co  $L_3$  (black squares) and Dy  $M_5$  (red circles) edges as a function of the pump – probe delay measured at  $T^* = 350\text{K}$  (a),  $400\text{K}$  (b) and  $540\text{K}$  (c). The solid lines are the fitting functions. The vertical blue dotted lines denote the delay at which the magnetization of the Co sublattices reach the minimal value.

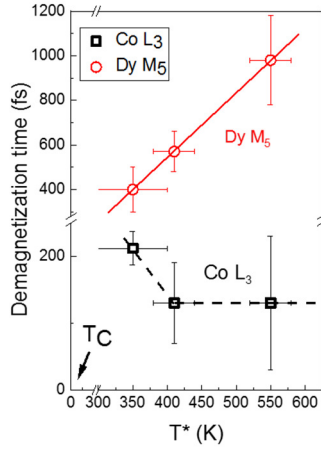


Figure 5: Characteristic demagnetization times for Co (black squares) and Dy (red circles) sublattices as a function of  $T^*$ . The error bars on the characteristic demagnetization times is given by the standard deviation from the fitting function. The error bars on the temperature were experimentally estimated (see text). The solid red line and dotted black line are guides for the eyes.

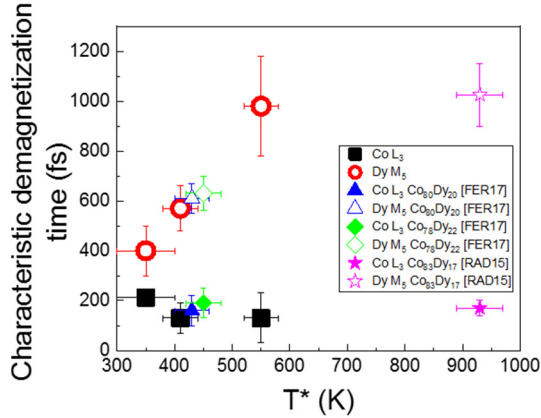


Figure 6: Characteristic demagnetization times for Co (filled symbols) and Dy (open symbols) sublattices as a function of  $T^*$ . We report our experimental results (black squares and red circles) superposed to published data extracted from element and time-resolved experiments performed on  $Co_{80}Dy_{20}$  (filled and empty blue triangles) [FER17],  $Co_{78}Dy_{22}$  (filled and empty green lozenges) [FER17] and  $Co_{83}Dy_{17}$  (filled and empty magenta stars) [RAD15].

### Acknowledgments:

We are indebted for the scientific and technical support given by N. Pontius, Ch. Schüßler-Langeheine and R. Mitzner at the slicing facility at the BESSY II storage ring. The authors are grateful for financial support received from the following agencies: the French “Agence Nationale de la Recherche” via Project No. ANR-11-LABX-0058\_NIE and Project EQUIPEX UNION No. ANR-10-EQPX-52, the CNRS-PICS program, the EU Contract Integrated Infrastructure Initiative I3 in FP6 Project No. R II 3CT-2004-50600008. Experiments were

carried out on the IJL Project TUBE-Davms equipment funded by FEDER (EU), PIA (Programme Investissement d'Avenir), Region Grand Est, Metropole Grand Nancy, and ICEEL.

The authors have no competing interests to declare

**References:**

- [BEA96] Beaupaire et al. Phys. Rev. Lett. 76, 4250 (1996)
- [KOO10] Koopmans et al. Nature Materials 9, 259 (2010)
- [BAT10] Battiato et al. Phys. Rev. Lett. 105, 027203 (2010)
- [CAR11] Carva et al. Phys. Rev. Lett. 107, 207201 (2011)
- [ESS12] Essert et al. J. Appl. Phys. 111, 07C514 (2012)
- [CAR13] Carva et al. Phys. Rev. B. 87, 184425 (2013)
- [SCH13] Schellekens et al. Appl. Phys. Lett. 102, 252408 (2013)
- [SHO17] Shokeen et al. Phys. Rev. Lett. 119, 107203 (2017)
- [STA07] Stamm et al. Nature Materials. 6, 740 (2007)
- [KUI11] Kuiper et al. J. Appl. Phys. 109, 07D316 (2011)
- [ROT12] Roth et al. PRX 2, 021006 (2012)
- [WIE11] Wietstruk et al. Phys. Rev. Lett. 106, 127401 (2011)
- [SUL12] Sultan et al. Phys. Rev. B. 85, 184407 (2012)
- [ESC14] Eschenlohr et al. Phys. Rev. B. 89, 214423 (2014)
- [FRI15] Frietsch et al. Nature Commun. 6, 9262 (2015)
- [RET16] Rettig et al. Phys. Rev. Lett. 116, 257202 (2016)
- [CHU06] Chubykalo-Fesenko et al. Phys. Rev. B 74, 094436 (2006)
- [MEN14] Mendil et al. Scientific Reports 4, 3980 (2014)
- [KIS00] Kise et al. Phys. Rev. Lett. 85, 1986 (2000)
- [MAN12] Manchon et al. Phys. Rev. B 85, 064408 (2012)
- [KIM14] Kimling et al. Phys. Rev. B 90, 224408 (2014)
- [BOB17] Bobowski et al. Journal of Phys. Cond. Matter. 29, 234003 (2017)
- [ATX12] Atxitia et al. Phys. Rev. B 86, 104414 (2012)
- [ATX14] Atxitia et al. Phys. Rev. B 89, 224421 (2014)
- [MOR17] Moreno et al. Phys. Rev. B 96, 014409 (2017)
- [MOR19] Moreno et al. Phys. Rev. B 99, 184401 (2019)
- [RAD15] Radu et al. SPIN, 5, 1550004 (2015)

[LOP13] Lopez-Flores et al. Phys. Rev. B 87, 214412 (2013)  
[RAD11] Radu et al. Nature. 472, 205 (2011)  
[GRA13] Graves et al. Nature Materials. 12, 293 (2013)  
[BER14] Bergeard et al. Nature Communications 5, 3466 (2014)  
[HIG16] Higley et al. Rev. of Sci. Instrum. 87, 033110 (2016)  
[FER17] Ferté et al. Phys. Rev. B 96, 134303 (2017)  
[HAN91] Hansen et al. J. Appl. Phys. 69, 3194 (1991)  
[HOL14] Holldack et al. J. Synchrotron Rad. 21, 1090 (2014)  
[MAN86] Mansuripur et al. IEEE trans. 22 33 (1986)  
[BER17] Bergeard et al. Phys. Rev. B 96, 064418 (2017)  
[DON17] Donges et al. Phys. Rev. B 96, 024412 (2017)  
[BIN06] Binder et al. Phys. Rev. B 74, 134404 (2006)  
[STA06] Stanciu et al. Phys. Rev. B 73, 220402 (2006).  
[BOE10] Boeglin et al. Nature, 465, 458 (2010)  
[LOP12] Lopez-Flores et al. Phys. Rev. B 86, 014424 (2012)  
[JAL19] Jal et al. Phys. Rev. B 99, 144305 (2019)  
[FRI16] Frietsch et al. Jpn. J. Appl. Phys. 55, 07MD02 (2016)  
[GAN18] Gang et al. Phys. Rev. B 97, 064412 (2018)  
[ATX11] Atxitia et al. Phys. Rev. B 84, 144414 (2011)  
[ZHE18] Zheng et al. Phys. Rev. B 98, 134409 (2018)  
[ATX18] Atxitia. Phys. Rev. B 98, 014417 (2018)  
[AND15] Andres et al. Phys. Rev. Lett. 115, 207404 (2015)  
[GOR18] Gort et al. Phys. Rev. Lett. 121, 087206 (2018)  
[HAA14] Haag et al. Phys. Rev. B 90, 134410 (2014)  
[BRO91] Brooks et al. Journal of Physics cond. Matter. 3, 2357 (1991)  
[FER17b] Ferté et al. Phys. Rev. B 96, 144427 (2017)  
[FER19] Ferté et al. Jour. Magn. And Magn. Mat. 485, 320 (2019)  
[HEN19] Hennecke et al. Phys. Rev. Lett. 122, 157202 (2019)  
[ATX11] Atxitia et al. Phys. Rev. B 84, 144414 (2011)  
[SCH13] Schellekens et al. Phys. Rev. B 87, 020407 (2013)  
[XU17] Xu et al. Advanced Materials. 29, 1703474 (2017)  
[IIA18] Iihama et al. Advanced Materials. 30, 1804004 (2018)